Sygnatura: © Pol J Radiol, 2007; 72(4): 7-20

Polish Journal of Radiology
www.PolRadiol.com
ORIGINAL ARTICLE

Otrzymano: 2007.01.23
Zaakceptowano: 2007.09.30

Value of MR examinations in diagnostics of cardiovascular diseases

Tomasz Harań, Zdzisława Bem

Lower Silesian Center of Diagnostic Imaging, Regional Specialist Hospital, Wrocław, Poland

Author's address: Tomasz Harań, Lower Silesian Center of Diagnostic Imaging, Regional Specialist Hospital, 53-204 Wrocław, Ojca Beyzyma 39, e-mail: haran@interia.pl

Summary

Background: Magnetic Resonance (MR) is one of the newest achievements in diagnostic medicine. Practical validation of MR in cardiovascular diseases is very important, due to growing interest of cardiologists in this method and information in literature about usefulness of MR in cardiology.

Material/Methods: In years 1996-2004, Lower Silesian Center of Diagnostic Imaging examined 134 patients with cardiovascular diseases with MR. Coarctation of the aorta (CoA) – 23 cases, patients after correction of the CoA – 17 cases, hypoplastic aortic arch – 5 cases, complex aortic arch abnormalities – 7 cases, congenital cardiac defects – 9 cases, patients after surgical correction of the heart defect – 12 cases, control after heart operation in an adult – 1 case, suspicion of arrhythmogenic right ventricular dysplasia (ARVD), myocarditis and cardiomyopathies – 32 cases, primary and secondary tumors of the heart – 4 cases, left ventricle aneurysms – 9 cases.

All the patients underwent USG examination, in 25 cases digital subtraction angiography (DSA) and hemodynamic examination were performed. In 6 cases CT of the chest was performed. Correlation between MR and USG, DSA, CT examinations was evaluated.

Results/Conclusions: In our material, the best results of MR examinations were achieved in diagnostics of the thoracic aorta disease. Measurements of the aorta diameter in MR strictly correlate with the results obtained in USG examination. In complex aortic arch abnormalities, MR seldom can replace DSA examination – only in easier cases, but it can help and reduce the time of DSA examination. MR may evaluate the pulmonary trunk and pulmonary vessels. MR perfectly visualizes morphology of the cardiac chambers, their spatial relationship, contractility and connection to great vessels. Assessment of septal defects and valves morphology in MR is inferior to USG examination. MR enables recognition of the ARVD. Less satisfactory results were obtained in diagnostics of myocarditis. MR is a perfect method of visualization and evaluation of cardiac tumors bigger than 5 mm.

Key words: **Magnetic resonance • heart • USG • aorta • coarctation of the aorta • pulmonary arteries • cardiac valves insufficiency • congenital heart defects • post-infarct left ventricle aneurysm • cardiomyopathy • arrhythmogenic right ventricle dysplasia**

PDF file: http://www.polradiol.com/fulltxt.php?ICID=510448

Background

Cardiovascular diseases are the most common cause of mortality in developed countries. The increasing epidemics of these disorders has led to rapid development of cardiology, cardiosurgery and related medical disciplines.

The search for more and more sophisticated diagnostic methods making it possible to diagnose and treat cardiovascular diseases is one of the directions of progress in cardiology.

Magnetic resonance is one of such methods. The first reports concerning application of magnetic resonance imaging (MRI) in cardiovascular diagnostics appeared in the early 1980's [1, 2]. The foundations for MRI use in cardiology were laid in 1970's by Damadian and Lauterbur. Lauterbur was the first to obtain an MR image of the heart in 1977. Good quality heart images, however, were not obtained until 1983 [1].

The aim of the study was to assess the usefulness of this method in clinical applications.

Materials and methods

In 1996-2004, in the Lower Silesian Center of Diagnostic Imaging of the Regional Specialist Hospital in Wrocław (Head: Prof. Zdzisława Bem, MD, Ph.D.) 134 patients diagnosed with cardiovascular diseases (CVD), including 86 males and 48 females, were examined with MR. The patients' age ranged from 5 days to 79 years, with the mean age value of 14.2 years. (table 1) Our material included 23 cases of aortic isthmus coarctation, 17 patients examined for control after surgical correction of aortic isthmus coarctation, 5 with aortic arch hypoplasia, 7 with complex thoracic aorta pathologies, 9 with congenital heart defects, 12 examined for control after surgical correction of congenital heart defects, 1 examined for control after cardiac surgery in adult age, 15 with suspected RVAD, 32 with myocarditis and cardiomyopathies, 4 with primary and secondary heart tumors, and 9 cases with post-infarction left ventricular aneurysms.

MRI was performed using Magnetom Impact 1,0T equipment (Siemens A.G.) before and after modernization of the system to Magnetom Harmony Maestro Class. The examinations were performed using ECG gating. In all the patients, imaging studies were performed in spin echo (SE) sequences, in T1-weighted sequences, in most patients also in T2-weighted sequences and in the CINE option in gradient echo sequence (FLASH and TRUE-FISP). Contrast medium (Omniscan or Magnevist, 0.1-0.2 mmol/kg b.w.) was administered to 34 patients.

All the patients had previously undergone heart USG, 25 digital subtraction angiography (DSA) and hemodynamic investigations. In 6 patients, CT of the thorax was additionally performed. Retrospective review of available medical records was carried out to confirm the diagnoses based on MR.

Statistical parameters

The information concerning the patients was collected on individual forms and then transferred to a computed database in the form of a table.

To assess the diagnostic value of MR, sensitivity, specificity and diagnostic efficiency indexes were calculated. The reference data in case of coarctation of the aorta were records of the surgery and DSA (in one case). The reference data in case of postoperative follow-up examinations included assessment of pressure gradient by Doppler sonography, DSA, CT of the thoracic cavity. In aortic arch hypoplasia, the reference examination was DSA along with intraoperative data and autopsy data. In patients with heart defects and after their surgical correction, the reference data included the results of heart USG and catheterization. In the group with cardiomyopathies and suspected myocarditis, clinical data, as well as the further course of the disease and autopsy findings, provided the most important diagnostic criteria. In case of cardiac tumors, MR images were compared with USG results, intraoperative findings, CT and autopsy data. For post-infarction left ventricular aneurysms, MR was compared with USG.

The particular categories of CVD were analyzed with respect to visualization of the leading pathology and coincident anomalies, detectable or not by MR. For the individual patient groups, the numbers and types of pathologies detected by MR and USG were recorded.

In smaller and heterogeneous groups, MR was assessed qualitatively with respect to usefulness in the diagnostics of particular pathology types.

Table 1. Age, sex and number of patients in analyzed groups of pathologies.

Pathology type	Total number	Males	Females	Age range	Mean age
Aortic isthmus coarctation	23	16	7	3 months-28 years	11.75
Control after CoAo surgery	17	11	6	1-20 years	10.7
Aortic arch hypoplasias	5	5	0	5-62 days	23 days
Complex thoracic aorta defects	7	5	2	3-15 years	10.86
Heart defects	9	5	4	2 months-12 years	7.47
Conditions after surgical cardiac defects correction	12	10	2	1-15 years	7.1
Post-surgery conditions in adults	1	1	0	77	77
Suspected ADPK	15	11	4	6-46 years	15.5
Myocarditis or cardiomyopathy	32	16	16	1 month-22 years	9.8
Primary and secondary heart tumors	4	0	4	1-46 years	23.5
Post-infarction left ventricular aneurysms	9	6	3	42-79 years	58.1
Total	134	86	48	5 days-79 years	14.2

The results were classified as:

- True positive (TP) – a pathology was found, which was confirmed by other diagnostic methods and clinically.
- True negative (TN) – no pathology was found, which was confirmed.
- False positive (FP) – a pathology was found, which was not confirmed.
- False negative (FN) – no pathology was found, but it was detected by other methods.

The results were presented in the form of a table. They provided a basis for calculation of sensitivity, specificity and diagnostic accuracy indexes:

Sensitivity: I_{se}= (1-FN/(TP+FN)) x100%

Specificity: I_{sp}= (1-FP/(TN+FP)) x100%

Accuracy: I_a=(TP+TN)/nx100%, where n – total number of examinations.

Evaluations:
- In the group of patients with aortic isthmus coarctation and after its surgical correction, visualization of the isthmus and the operation site in MR and USG was evaluated.
- Consistency of aortic bulb diameter measurements obtained in MR and USG. Pearson's linear correlation coefficient was calculated for these data. The data were compared because the aortic bulb diameter is always accessible in USG and measurement accuracy obtained with USG of this region is very good. By obtaining high correlation between aortic bulb diameter measurements in MR and USG, we confirm the accuracy of measurements of other aortic segments in MR.
- The correlation between the pressure gradient in the coarctation site noted on USG with the grade of stenosis found in MR in patients after surgical correction of aortic isthmus coarctation was examined. The stenosis grade was expressed as the ratio of isthmus diameter (I) to descending aorta diameter (D). The correlation between the pressure gradient in the coarctation site with the **I/D** ratio was tested.

Pearson's linear correlation coefficient was calculated for the compared values.

Pearson's linear correlation coefficient:

$$r_{xy} = \frac{\sum_{i=1}^{n}(x_i - \bar{x})(y_i - \bar{y})}{\sqrt{\sum_{i=1}^{n}(x_i - \bar{x})^2 (y_i - \bar{y})}}$$

Where:
x_i, y_i – variants of the parameter.

$\bar{x}$, $\bar{y}$ – arithmetic means.

In the case of low linear correlation, Spearman's rank correlation coefficient was also calculated.

Spearman's rank correlation coefficient:

$$r_s = 1 - \frac{6\sum_{i=1}^{n} d_i^2}{n(n^2 - 1)}$$

Where:
d_i = differences between ranks of the corresponding values of the x_i and y_i parameter (i = 1,2, … , n).

x_i, y_i – variants of the parameter.

$\bar{x}$, $\bar{y}$ – arithmetic means.

n – sample size.

- In all patient groups, coincident cardiovascular abnormalities detected by MR and USG were compared
- In the group of patients with complex aortic arch anomalies, the position of MR among other diagnostic methods was assessed.
- In case of hypoplastic aortic arch, the number of anomalies visualized correctly in MRI, and the degree of visualization in MRI and USG of the coincident abnormalities were analyzed.
- Effectiveness of magnetic resonance in myocardial signal assessment in the group of patients with RVAD, myocarditis and cardiomyopathy diagnoses vas evaluated.
- The usefulness of MR in detection of cardiac and mediastinal tumors was assessed. The degree of visualization of the pathologies and information contributed by MRI was analyzed.
- In the group of patients with post-infarction left ventricular aneurysms, the correlations between measurements of the left ventricle and aneurysm volume obtained in MR and USG were analyzed. Additionally, the subjective criterion of the ease of assessment of the pathologies in MR and USG was evaluated.

Results

Magnetic resonance allowed to visualize the shape and diameter of the aortic isthmus in all 23 cases, whereas in USG the aortic isthmus was visualized in 3 children only (table 2).

In 22 cases, coarctation of the aortic isthmus was detected in MR.

In 1 case, MR excluded the presence of coarctation. 100% of true positive and 100% of true negative results was obtained. The sensitivity, specificity and accuracy indexes equaled 100%.

In the group of patients examined after surgical correction of aortic coarctations, MR visualized the operation

Table 2. Estimation of morphology of coarctation of the aortic isthmus.

No	Initials	Coarctation type visualized in MR	Coarctation type visualized in USG
1.	J.M	Hourglass type, in further part membranous	Only the initial segment of the coarctation visualized, other parts invisible
2.	D.N.	Aortic isthmus coarctation excluded	Suspected coartctation
3.	G.T.	Membranous type	Not visualized
4.	D.A.	Membranous	Not visualized
5.	S.S.	Membranous	Not visualized
6.	G.B.	Elongation of the aortic arch and hourglass-like isthmus coarctation	Not visualized
7.	S.M.	Mild, hourglass-like	Not visualized
8.	S.A.	Membranous type with geniculate bend	Not visualized
9.	K.M.	Hourglass type	Not visualized
10.	G.P.	Membranous type	Not visualized
11.	CH.D.	Membranous type + hourglass-like stenosis	Not visualized
12.	J.M.	Membranous type, mild aortic arch hypoplasia	Not visualized
13.	S.M.	Membranous	Not visualized
14.	W.M	Membranous	Membranous with visible morphology
15.	M.M.	Membranous + aortic arch hypoplasia	Not visualized
16.	O.M.	Membranous	Not visualized

sites in all the cases. The presence of residual stenosis was observed in 9 patients. The presence of stenosis was confirmed by USG finding of pressure gradient in 8 cases.

The correlation of aortic isthmus to descending aorta diameter (measured at the level of the diaphragm) – I/D with the presure gradient observed in Doppler sonography was analyzed. The results of the calculations are presented in tables 3 and 4.

For both patient groups, the consistency of aortic bulb diameter measurements in USG and MR was assessed. Very high consistency of the compared results was observed (graph 1).

Another group consisted of 7 patients with more complex aortic arch anomalies. In this group, the position of MR among other diagnostic examinations was assessed. In 5 cases, MR played an important role in diagnostics and revealed the majority of pathologic changes, in 2 cases, it was the most important diagnostic method, allowing ultimate determination of morphology of the anomaly.

In the group of 5 patients with hypoplasia of the aortic arch, morphology of the anomaly was visualized very well in 4 cases and well in 1.

Then, collective analysis of all the cases of coarctation of the aorta and heart defects with respect to the detected

Table 3. Examination of linear correlation.

Initials	I/D index: ratio of the surgical site diameter to diameter of the descending aorta at the diaphragm level	Presence of restenosis in USG (pressure gradient [mmHg])
M.M.	0.73	18
N.K.	0.69	27
K.M.	0.69	28
C.A.	0.85	35
C.A. Child re-examined after 4 years	0.54	35
Ch.D.	0.67	20
Ch.D. Child re-examined after 4 years	0.61	40
S.S.	0.64	35
Pearson's coefficient for I/D and gradient: 0.213550408. This indicates very weak linear correlation.		

Table 4. Values of attributes and variables applied in calculation of Spearman's rank correlation coefficient.

Initials	ID index	I/D rank	Pressure gradient [mm Hg]	Gradient rank	d_i	d_i^2
M.M.	0.73	2	18	1	1	1
N.K.	0.69	3.5	27	3	0.5	0.25
K.M.	0.69	3.5	28	4	-0.5	0.25
C.A.	0.85	1	35	6	-5	25
C.A. Child re-examined.	0.54	8	35	6	2	4
Ch.D.	0.67	5	20	2	3	9
Ch.D. Child re-examined.	0.61	7	40	8	-1	1
S.S.	0.64	6	35	6	0	0
Spearman's rank correlation coefficient = 0.48 indicates moderate positive correlation of the analyzed parameters.						

pathologies located both in the heart and in the large vascular trunks was carried out (tables 5, 6, 7, 8).

The following results were obtained:

Assessment of MR usefulness in the presented group:

- MR shows the location of the heart in relation to other mediastinal structures
- The size of cardiac chambers and the thickness of the myocardium can be assessed.
- Larger atrial and ventricular septal defects are visible.
- Collateral circulation is visible well in case of coarctation of the aorta.
- MR ensures good visualization of right ventricular blood outflow tract.
- MR is useful in assessment of the pulmonary artery trunk and its main branches.
- In case of pulmonary vascular hypoplasia, only the collaterals arising from the aorta and supplying the pulmonary interstitium with blood are visible.
- MR shows the morphology of the pulmonary trunk and the aorta origination sites before and after surgical transposition of the large vessels.
- Assessment of homograft of the pulmonary artery is possible.
- It is possible to visualize surgical system to pulmonary shunts providing blood supply fom the subclavian arteries to the pulmonary vessels.
- Morphology of the vena cava is well visible.
- With MR, it is possible to assess the morphology of blood vessels arising from the aortic arch and exclude the presence of vascular rings causing the compression of the trachea and esophagus.
- The thoracic aorta is visible clearly.
- Visceral transposition can be visualized.

On the basis of the analyzed group of patients, the limirations of MR can be characterized as follows:

- There are problems with assessment of competence and function of cardiac valves.
- Poor visibility or failure to visualize smaller septal defects.
- Assessment of tightness of the patches used for repair of these defects is impossible.
- Magnetic resonance is less precise than conventional angiography in assessment of the pulmonary vessels and collateral circulation in the cases of pulmonary arterial hypoplasia.
- Our material included non-diagnostic results, when considerable arrhythmias or no cooperation on the patient's part made it difficult or impossible to perform the examination.

The next group of patients consisted of children referred for the examination in order to obtain myocardial signal assessment: 15 cases of suspected arrhythmogenic right ventricular dysplasia and 32 cases with suspicion of myocarditis or cardiomyopathy. Both groups were subjected to

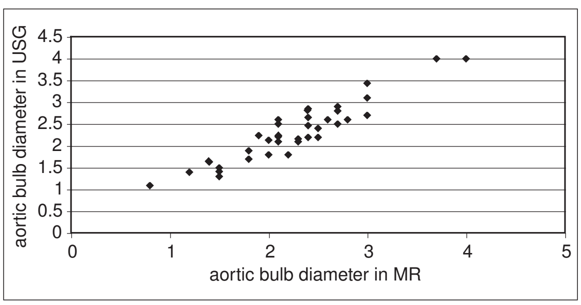

Diagram 1. Correlation of measurements of the aortic bulb diameter in USG and MR.

Table 5. Comparison of additional pathologies discovered in patients with coarctation of the aortic isthmus.

No	Pathology type	Number of abnormalities detected in MR	Number of abnormalities detected in USG
1.	Collateral circulation	6	0
2.	Complex aortic arch anomalies	4	0
3.	Left ventricular myocardial hypertrophy	5	8
4.	Mitral valve insufficiency	0	2
5.	Aortal valve insufficiency	0	6
6.	Tricuspid valve insufficiency	0	2
7.	Thickening or anomalies of the valve leaflets	0	6
8.	Atrial septal defect	0	2
9.	Ventricular septal defect	0	4
10.	Patent arterial duct	0	1

Table 6. Comparison of additional pathologies discovered in patients after surgical correction of the coarctation of the aortic isthmus.

Pathology type	Number of abnormalities detected in MR	Number of abnormalities detected in USG
Tortuous aorta	4	3
Hourglass-like bulb shape	1	1
Collateral circulation	1	0
Aortic arch anomalies	2	0
Left ventricular hypertrophy	1	1
Aortal valve insufficiency	0	1
Mitral valve insufficiency	0	3
Tricuspid valve insufficiency	0	1
Defects of the valve system	0	2
Left ventricular outflow stenosis	0	1

the same protocols with respect to the imaging technique and assessment of myocardial signal, and these 47 cases were analyzed collectively.

For arrhythmogenic right ventricular dysplasia, the obtained sensitivity index was 67%, specificity index – 100% and accuracy index – 96%.

For myocarditis, the obtained sensitivity index was 46%, specificity index – 82% and accuracy index – 72%.

For dilated cardiomyopathy, the obtained sensitivity index was 80%, specificity index – 93% and accuracy index – 89%.

For hypertrophic cardiomyopathy, the obtained sensitivity index was 100%, specificity index – 100% and accuracy index – 98%.

Table 7. Comparison of additional pathologies discovered in patients with hypoplasia of the aortic arch.

Pathology type	Number of abnormalities detected in MR	Number of abnormalities detected in USG
Arterial duct patency	2	1
Ventricular septal defect	1	2
Atrial septal defect	1	2
Subvalvular coarctation of aorta	1	1
Mitral valve insufficiency	0	1
Tricuspid valve insufficiency	0	2
Cardiac chambers enlargement	2	2

Analysis of 4 cases of mediastinal or cardiac tumors as also carried out. Pathology visualization quality and information contributed by MR were taken into consideration: the group consisted of 2 patients with small endocardial nodules, protruding into the ventricular or atrial lumen, 1 patient with a lymphoma infiltrating the heart, and 1 patient with a thymoma surrounding the left and right margin of the heart contour. Both the lymphoma and the thymoma were visible well, the examination was useful and contributed new clinical information, inaccessible by other investigations. In case of small endocardial nodules, MR was completely ineffective in 1 patient, and in the other patient, only 1 out of 3 nodules present could be visualized. The lesion was markedly enhanced after contrast medium administration.

Patients with post-infarction left ventricular aneurysms constituted the next group. The correlations between MR and USG measurements of the following parameters: left ventricular end-diastolic volume (EDV) and end-systolic volume (ESV) (diagram 2 and 3) and the aneurysm volume (diagram 6) were assessed here. Very good consistency of the measurements was obtained.

Table 8. Comparison of pathologies discovered in MR and USG in patients with congenital heart defects and after surgical correction of the disease.

Pathology type	Visualized in MR	Visualized in USG
Heart position in relation to other mediastinal and abdominal structures	21, better visualization of vena cava superior	21
Size and shape of cardiac chambers	21	21
Right ventricular outflow tract	21	21
Pulmonary trunk and its main branches	21	10, frequently only the pulmonary artery visible, vith poor visualization of its branches.
Homograft of the pulmonary artery	3, longer segment visible together with pulmonary vessels. Poorer visualization of the homograft valve.	3
Origin of the Aorta and pulmonary trunk	21	21
Collateral vascularization in case of pulmonary trunk hypoplasia and coarctation of aorta	1	1
Systemopulmonary shunts	2	0
Vascular anomalies – presence of vascular rings	1	1
Atrial and ventricular septal defects	4	10
Patches repairing septal defects	0	12
Valvular pathologies	3	36
Non-diagnostic examinations	1	0

An additional subjective criterion of detection ease with respect to abnormalities investigated by MR and USG was evaluated. Both the ventricular shape and the aneurysm morphology were better visible in MR. Fresh blood clots were less visible in MR than in USG – they were difficult to distinguish from the blood present in the aneurysmal lumen.

Discussion

Magnetic resonance of the heart is a fascinating modality from the border of radiology and cardiology. Cardio-MR is undoubtedly a more difficult task than other classic MR applications. The investigator's experience and familiarity with specialist software plays an essential role in obtaining reproducible and reliable results. USG is a relatively simpler method, which has been used for years in cardiac examinations. As emphasized by many authors, USG is subjective to some extent and the obtained results are dependent on interpretation of the images – especially with respect to the volume of the cardiac chambers.

Numerous publications emphasize the accuracy and reproducibility of heart MRI [3, 4]. However, the manner in which the scan is performed influences the results. It is emphasized in the literature that the results of MRI are dependent on the person planning the investigation, i.e. the subjectivity of the method has been shifted from the investigator interpreting the results to the person actually performing the scan. Therefore, it is very important to set the standards, to specify the sequence parameters, and to

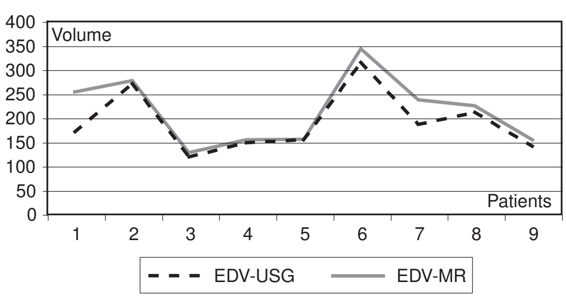

Pearson's coefficient for left ventricular EDV measured in USG and MR: 0.926517
Very strong linear correlation

Diagram 2. Left ventricle end diastolic volume measured in USG and MR.

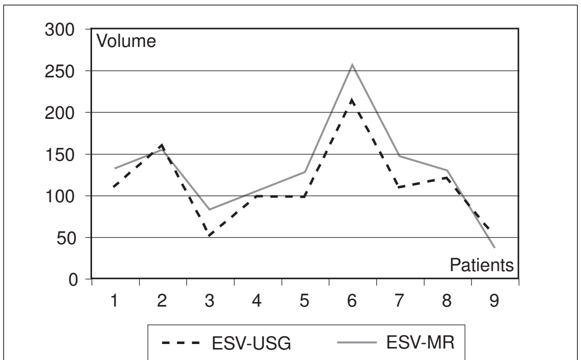

Pearson's coefficient for left ventricular EDV measured in USG and MR: 0.949707
Very strong linear correlation

Diagram 3. Left ventricle end systolic volume measured in USG and MR.

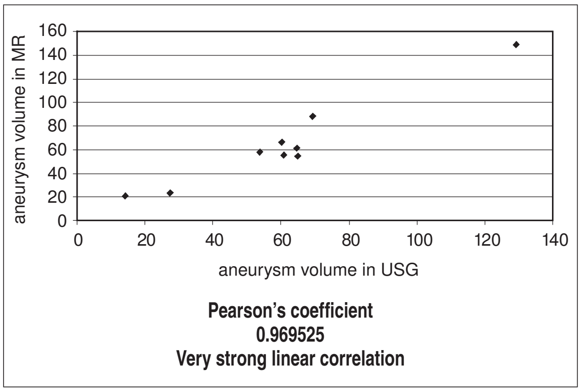

Diagram 4. Volume of the aneurysm in USG/ volume of the aneurysm in MR.

provide continuous training for the operators of MR equipment used in examinations of the heart.

The study design involved retrospective assessment of cardiac examinations performed during the last decade. In this period, MR techniques have undergone considerable changes. New sequences, allowing to investigate the previously inaccessible structures, such as the cardiac valves, have been introduced. The assessment of the obtained results in the aspect of MR usefulness in cardiological diagnostics must be presented in the context of new opportunities which have emerged during the recent years.

Coarctation of aorta and postoperative control

Diagnostics of aortic isthmus coarctation is based primarily on investigation of aortic morphology in USG and search for the effect of accelerated blood flow at the narrowed site. However, Doppler method is associated with some limitations. Marked increases of blood flow velocity without the presence of stenosis and with negligible pressure gradient between the upper and the lower extremity have been observed. It is associated with the dependence of pressure gradient and blood flow velocity at the stenosed site on susceptibility and elasticity of the ascending aorta and of the surgical site [5, 6, 7, 8, 9]. It is usually impossible to assess the morphology and to visualize the stenosis itself on the basis of two-dimensional USG, due to poor ultrasound penetration in the isthmus region [7, 10, 11, 12, 13]. In the past, accurate assessment of aortic isthmus morphology could be obtained by conventional methods making use of digital subtraction angiography (DSA). Now, the recently introduced MR techniques for examination of the aorta have almost completely replaced classic angiography in the diagnostics of this disease [14]. Numerous authors [13, 14, 15, 16, 17, 18, 19, 20, 21, 22, 23, 24, 25, 26, 27] demonstrate high sensitivity and specificity of MR in the diagnostics of aortic anomalies. In our laboratory, very high sensitivity and specificity of the method was obtained with respect to detection of aortic isthmus coarctations and grading of these defects (figure 1). Measurement of the aortic diameter, precise assessment of the morphology of isthmus coarctation and of the course of the left subclavian artery are indispensable for planning surgical treatment and technique of the procedure. This is why we consider the accuracy of measurements obtained by MR and USG so important. We were most interested in the accuracy and reliability of coarctation site measurements. We decided to assess them in an indirect way, by comparing the results of MR and USG concerning the diameter of the aortic bulb. The results obtained with both methods were highly consistent. It is noteworthy that the values obtained in MR were usually slightly lower than those obtained in USG. In can be explained by differences in the measurement techniques – in MR the image used for measurements was averaged on the basis of many cardiac evolutions [28], whereas in USG the diameter of the blood vessel recorded in the specific moment of the examination was measured.

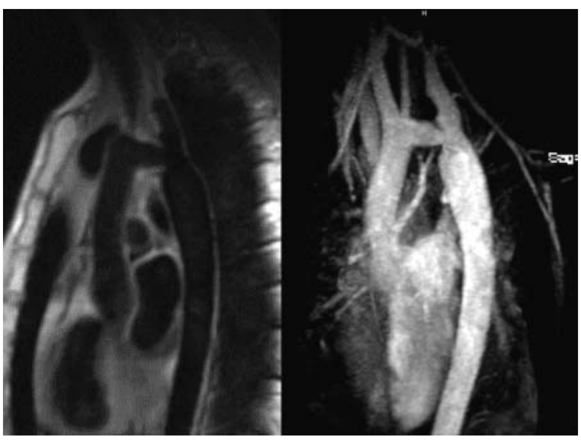

Figure 1. A patient after surgical correction of the aorta coarctation. Residual stenosis is visible in T1-weighted images and in MR angiography.

It was checked whether there was a correlation between the grade of residual stenosis of the aorta in patients after surgical correction of aortic coarctation and the pressure gradient recorded at that site in USG.

Analysis of the obtained results demonstrated only moderate correlation of these values – no linear correlation of the compared data could be demonstrated, with their weak positive correlation: Spearman's correlation rank coefficient value was 0.48. Our results seem to be logical, because the gradient of pressures at the surgery site is determined by many factors, such as left ventricular ejection volume, aortic wall elasticity, and it cannot be in linear correlation with the coarctation grade; however, some correlation should be visible.

On the basis of the obtained results, an opposite conclusion can be made as well: the residual stenosis grade cannot be estimated only on the basis of pressure gradient detected in USG.

Complex aortic abnormalities

All the cases of congenital complex aortic arch abnormalities and secondary complex anomalies of the thoracic aorta were analyzed retrospectively.

The results of MR were compared with angiography.

Analysis of MR finings and their comparison with DSA images leads to a fundamental conclusion, that in case

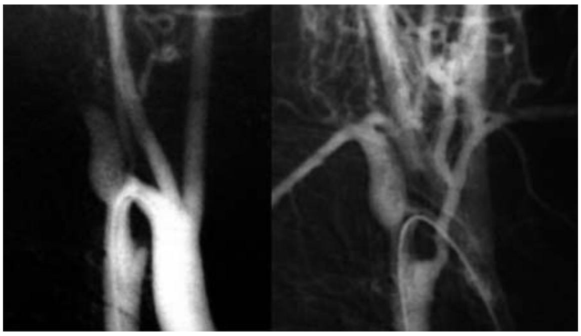

Figure 2. DSA examination. Right-sided aortic arch with coarctation of the aortic isthmus and abnormal origin of the cephalad vessels. Steal syndrome. Two sequences are visible: early with contrast in aortic arch and late with contrast filling the subclavian arteries and the descending aorta through the vertebral arteries.

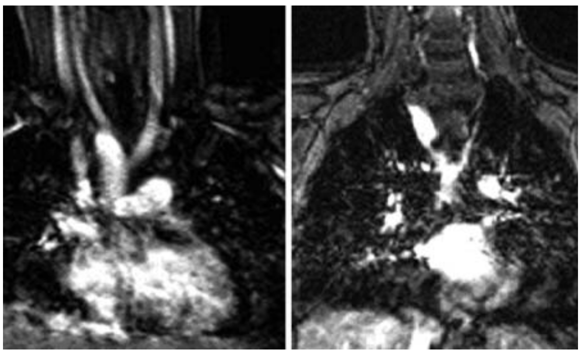

Figure 4. The same patient. In MR angiography in one projection, two cervical arteries are visible; in the second projection, vertebral arteries originating from the descending aorta are visible.

of complex aortic arch abnormalities MR can be treated only as a preliminary examination which precedes classic angiography (fig. 2, 3, 4). In simpler cases, MR can be performed instead of angiography (fig. 5).

Heart defects and other cardiovascular anomalies

Among the analyzed 134 cases, various cardiovascular defects or anomalies were detected in 73 patients. In 9, MR was performed to assess the diagnosed heart defects, whereas 12 were examined to control the effects of surgical correction of congenital heart defects. The analyzed patients did not constitute a homogeneous group. However, certain regularities could be observed.

Magnetic resonance allowed good visualization of anatomic relations inside the thoracic cavity, especially with respect to the relations between the heart and the other mediastinal structures, as well as the abdominal viscera.

Assessment of size and arrangement of the cardiac chambers was possible in MRI [29-31].

Collateral circulation was visualized well in the cases of anomalies affecting the large vascular trunks – both collateral circulation developed in coarctation of the aorta and the systemic circulation blood supply to the lungs in the cases of hypoplasia of the pulmonary vessels.

Figure 3. The same patient. TOF angiography of the cephalad arteries in MR.

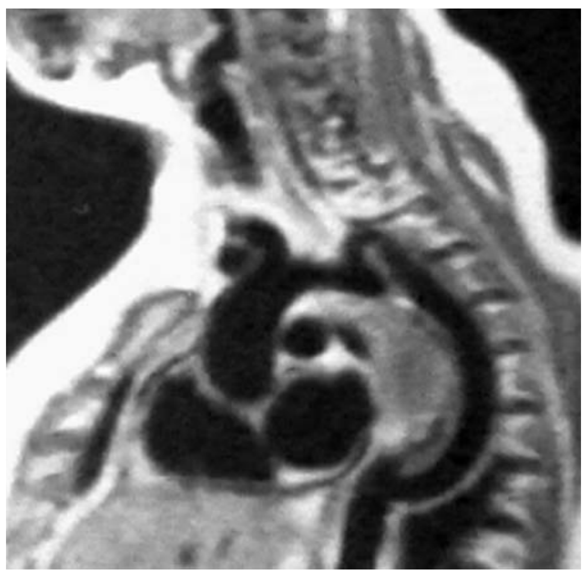

Figure 5. A patient with aorta coarctation and with a big postenotic aneurysm, after bypass grafting. A thrombosed aneurysm behind the stenosis site visible.

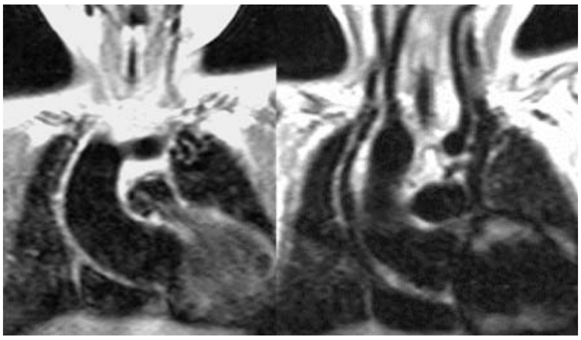

Figure 6. Coronal view, right-sided aortic arch running in a sagital plane. Widened ascending aorta, partial dupplication of the aortic arch with abnormal left subclavian artery.

Atypical origin of the cephalad arteries was also visualized (fig. 6, 7).

In the cases of Fallot tetralogy (fig. 8) MR allowed good visualization of right ventricular morphology – particularly the outflow tract and the relation between the aorta and the ventricular septum. Ventricular septal defects are usually clearly visible.

In case of control examinations after complete surgical correction of Fallot tetralogy, the examinations were performed to visualize the morphology and size of the right ventricle (fig. 9) its outflow tract (fig. 10), diameter of the pulmonary trunk, or its homograft [32-37]. MR visualized accurately the grade of myocardial hypertrophy of the right ventricle and its function. In out material, MR was inferior to USG as far as imaging of pulmonary valve insufficiency was concerned.

Imaging of pathologies of the valvular system was significantly worse or ineffective: thickening of valvular leaflets, as well as mild or moderate insufficiency of the cardiac valves were not demonstrated in our material. Only severe insufficiency was visible as retrograde blood flow in the FLASH sequence. Valvular system incompetence could also be detected indirectly on the basis of dimensions of the cardiac chambers.

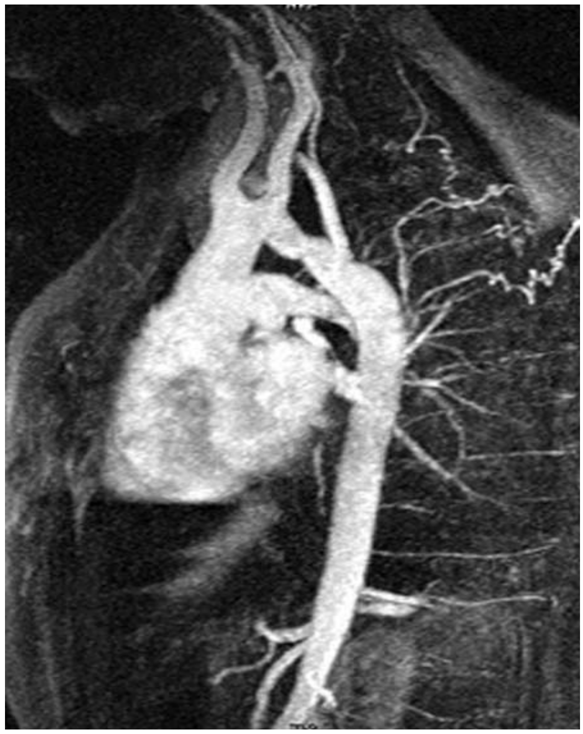

Figure 7. Coarctation of the aorta with abnormal right subclavian artery – arteria lusoria.

Atrial and ventricular septal defects caused considerable diagnostic problems – only larger anomalies were visualized.

In T1- and T2-weighted projections it was impossible to visualize dacron patches covering the defects. Direct assessment of patch tightness was also impossible.

Figure 8. Tetralogy of Fallot. The right ventricle outlet and the aortic bulb are visible.

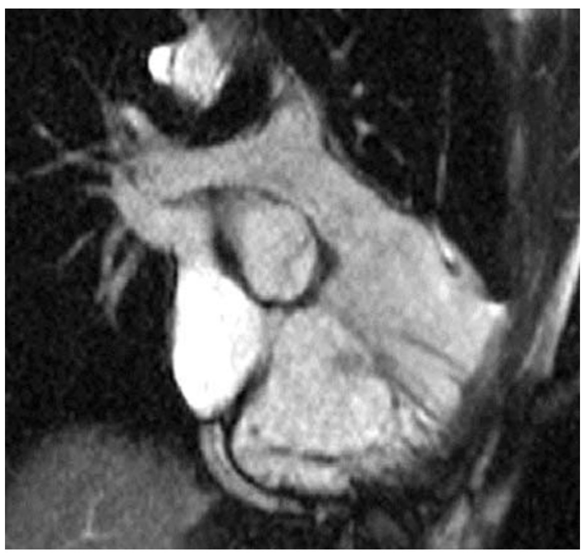

Figure 9. True FISP sequence, Four-chamber view. A patient after correction of the tetralogy of Fallot. Right ventricle enlargement due to pulmonary valve insufficiency.

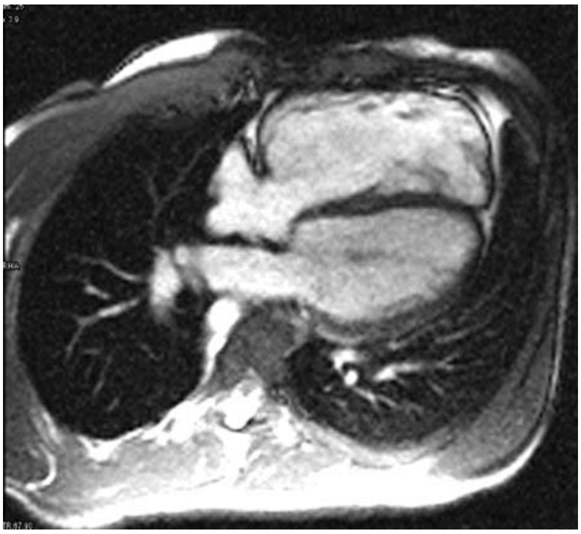

Figure 10. The same patient as in figure 13. True FISP sequence, view showing the tricuspid valve, the right ventricle outlet tract, the pulmonary trunk and both pulmonary arteries.

The pulmonary trunk together with the right and left pulmonary arteries, even markedly hypoplastic, was visualized very well. However, further segments of the pulmonary arteries were better visible in DSA.

Patients with suspected myocarditis or cardiomyopathy

In patients referred for dignostics with suspected myocardial abnormalities, the investigations were performed in an identical manner, irrespective of whether the diagnosed abnormality was myocarditis, arrhythmogenic dysplasia, or cardiomyopathy. Imaging was performed in T1- and T2-weighted sequences, and in the cases of suspected myocarditis, contrast-enhanced images were also obtained. Considering the uniform procedure and similarity of the clinical data, the whole material available was subjected to statistical analysis concerning the diagnostic usefulness of MR in the aforementioned diseases.

Right ventricular arrhythmogenic dysplasia (RVAD) is characterized by morphological abnormalities of the ventricular wall. The most characteristic feature is replacement of the myocardium by adipose, or adipose and fibrous tissue (fig. 11) with local disturbances of contractility. Because of tissue specificity of the MR signal, this method is useful in the diagnostics of this entity [38-41].

MR has been proven to be a specific method in the diagnostics of RVAD (the specificity index equalled 100%), but characterized by low sensitivity – 67%. However, no statistical significance was reached because of small number of clinically confirmed cases of this pathology – only 3.

In the diagnostics of myocarditis, MR demonstrated low sensitivity – 46%, good specificity – 82% and 73% accuracy.

In our opinion, such results are not satisfactory. Low sensitivity is determined by clinical conditions and cardiological examination software currently available in our center. The diagnosis of myocarditis was established on the basis of

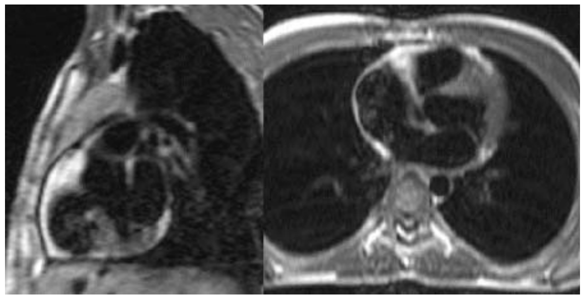

Figure 11. A patient with cardiac arrhythmia of right ventricular origin, ADPK suspected. Oblique and transverse section. T1/SE sequences. Intense bright signal from the right ventricle outlet tract and free wall, suggesting fatty infiltration. Bright signal is also visible on the border between the left atrium and left ventricle.

T2-weighted images (fig. 12), and the grade of contrast enhancement of the myocardium. The failure of our assessment is associated with the fact that it was difficult to obtain good quality T2-weighted images especially in the cases of concurrent arrhythmias. In T2-weighted sequences, numerous artifacts are present, among which the most misleading one was subendocardial signal increase due to averaging of the myocardial and hyperintense immobile blood on the periphery of the cardiac chamber. The above phenomena had a negative effect primarily on the number of false positive diagnoses of inflammatory changes in healthy children.

Literature reports indicate high diagnostic value of MR in myocarditis-related changes [42].

The reasons for the discrepancy between the results obtained in our study and the literature data were as follows:

First, shortcomings of the equipment – T2-weighted images obtained in the studied group of patients were of too low quality.

Second, the studied group of patients was too heterogeneous – it consisted of children with different clinical stages of the pathology.

Figure 12. A patient with diagnosed myocarditis. Transversal view, SE, T2-weighted sequence. Irregularly elevated signal is visible from the heart muscle of the posterior left ventricle wall.

Figure 13. Transversal view. SE, T1-weighted sequence. A small nodule originating from the septal wall is visible in the right ventricle, on the border with tricuspid valve.

Third, the diagnosis of myocarditis in some children was confirmed by clinical data only, regression of symptoms and increased titer of antibodies against viruses from the Coxackie group. No uniform diagnostic criteria were applied. In view of the above, the ultimate diagnoses established in some children treated on outpatient basis were not reliable.

Tumors of the heart

The diagnostic value of MR in this entity is dependent on the lesion and conditions of the examination. If the existing pathology is very small – below 0.5cm in diameter, and localized between the myocardial trabeculae or on the valvular leaflets, it may be difficult to find and differentiate from the muscle tissue, especially in T1-weighted images [43, 44]. We observed a case of a child with 3 nodules described in USG. In MR, only one of them was visible and enhanced after contrast administration (fig. 13). In our material, extensive infiltration of the heart and blood vessels was visualized very well in a case of lymphoma (fig. 14). MR also showed correctly a lesion of thymoma type, enclosing the heart (fig. 15).

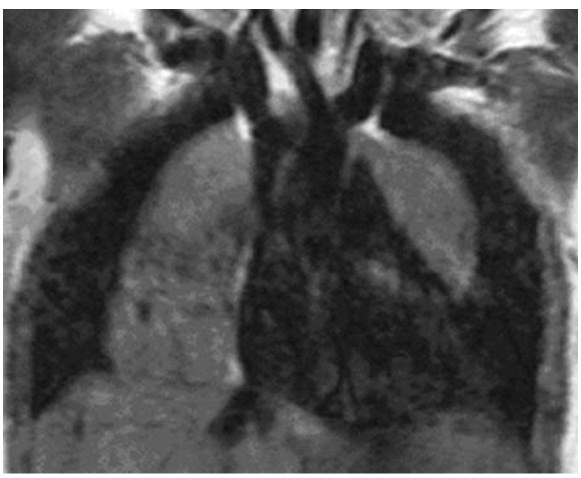

Figure 15. Coronal section. Examination in SE, T1-weighted sequence. A tumor around the right and left border of the heart.

Figure 14. Transversal section. SE, T1-weighted sequence. A tumor of the posterior mediastinum, infiltrating the left atrium and posterior wall of the left ventricle.

Post-infarction left ventricular aneurysms

The consistency of left ventricular systolic and diastolic valume measurements performed using MR and USG was analyzed. In accordance with the data reported in the literature, very good correlation of these results was demonstrated.

MR was superior to USG with respect to the possibility of aneurysmal morphology visualization, because of no limitations imposed by the accoustic window and the possibility of multiplanar presentations (fig. 16, 17). MR visualized very well the presence of thrombi within the aneurysms (fig. 18, 19). Fresh blood clots demonstrated poorer differentiation from blood trapped within the aneurysm in gradient echo images, and, consequently, poorer visibility.

In many situations, MR provides an alternative for USG, especially in the cases in which USG is technically difficult to be performed, or the parameters of ventricular function must be measured in an objective and reproducible manner, e.g. for scientific purposes.

Conclusions

1. Recent advances in the MR techniques and software have contributed to the increasing role of this imaging modality in the diagnostics of diseases of the heart and large vascular trunks. The results of own studies confirm this opinion.

2. In the analyzed group of patients, the best results were obtained in examinations of the thoracic aorta. MR enabled complex assessment of the aorta superior to the results obtained with USG, and equivalent with angiography. The measurements of diameters of various aortic segments obtained in MR are closely correlated and consistent with measurements performed in USG. This

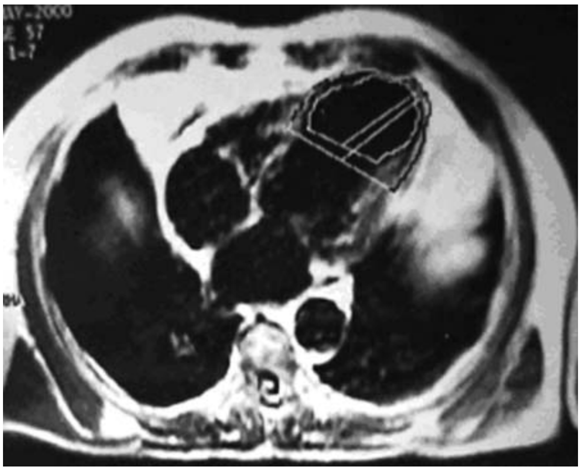

Figure 16. Four-chamber view, SE, T1-weighted sequence. Marked borders of the left ventricle aneurysm.

indirectly supports the claim concerning high accurracy of MR measurements of the aortic isthmus, inaccessible by USG.

3. MR allowed to establish 100% correct diagnoses of coarctation of the aorta and accurate assessment of the coarctation morphology. However, the assessment of coincident cardiovascular pathologies in these patients was more accurate in USG.

4. MR proved to be a very good method for monitoring the patients after surgical correction of aortic isthmus coarctation.

5. In complex aortic arh defects, MR can replace angiography only in simpler cases, whereas in more complicated ones it can reduce the time needed for catheterization of the heart.

6. MR can be used in assessment of the pulmonary arterial trunk and pulmonary vessels in patients with heart defects and pulmonary vascular hypoplasia.

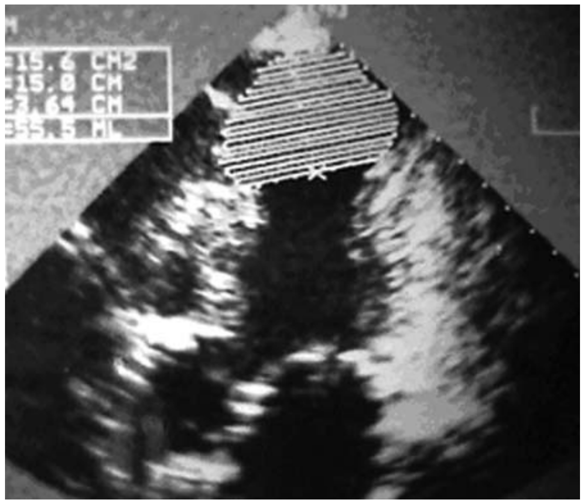

Figure 17. USG examination, four-chamber view. Marked borders of the left ventricle aneurysm.

7. MR provides excellent visualization of the structure, contractility, and mutual spatial relationships between the cardiac chambers and their junctions with the large vascular trunks. On the other hand, USG was found to allow more precise assessment of septal defects and valvular morphology.

8. MR allows to establish the diagnosis of arrhythmogenic right ventricular dysplasia. Worse results obtained with respect to assessment of myocarditis can be explained by too low standard of the equipment and cardiological software in the previously used device.

9. MR is and excellent method of diagnostics and assessment of heart tumors above 5mm and their differentiation from thrombi.

10. MR proved to be more accurate than USG in the assessment of post-infarction aneurysms of the left ventricle.

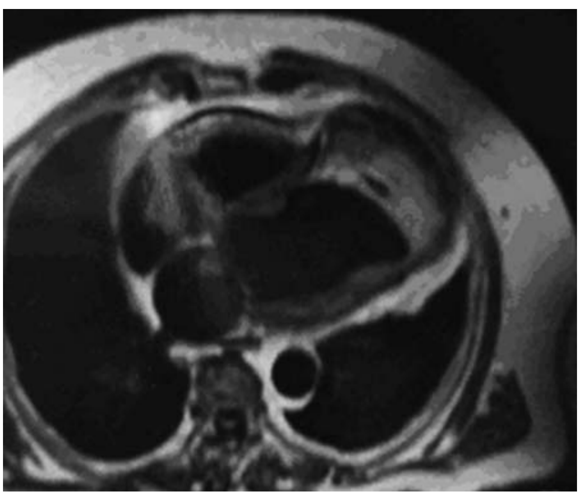

Figure 18. Transversal view, SE, T1-weighted sequence. A thrombus in the left ventricle aneurysm is clearly visible.

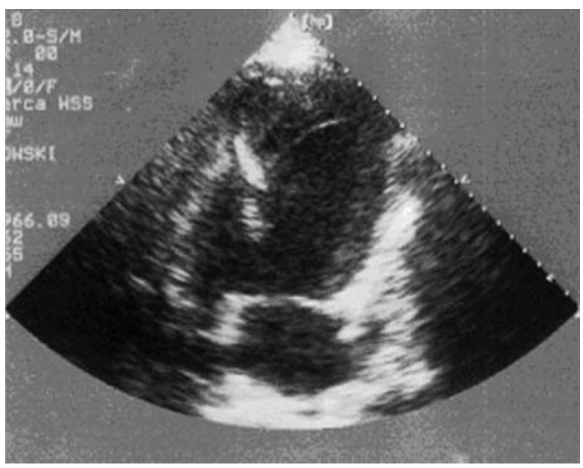

Figure 19. The same patient. USG examination, four-chamber view. Presence of the thrombus in the lumen of the left ventricle aneurysm.

References:

1. Herfkens RJ, Higgins CB, Hricak H, et al.: Nuclear magnetic resonance imaging of the cardiovascular system: normal and pathologic findings. Radiology (1983) 147: 749–759.
2. McNamara MT, Higgins CB: Cardiovascular applications of magnetic resonance imaging. Magn Reson Imaging (1984) 2:167–186.
3. Fogel MA: Assessment of Cardiac Function by Magnetic Resonance Imaging Pediatr Cardiol 2000; 21: 59–69.
4. Helbing WA, Bosch HG, Maliepaard C, et al.: Comparison of echocardiographic methods with magnetic resonance imaging for assessment of right ventricular function in children. Am J Cardiol (1995) 76: 589–594.
5. De Groff CG, Orlando W, Shandas R: Insights into the effect of aortic compliance on Doppler diastolic flow patterns seen in coarctation of the aorta: a numeric study. J Am Soc Echocardiogr 2003 Feb; 16(2): 162–9.
6. De Mey S, Segers P, Coomans I, et al.: Limitations of Doppler echocardiography for the post-operative evaluation of aortic coarctation. J Biomech 2001 Jul; 34(7): 951–60.
7. Lim DS; Ralston MA: Echocardiographic indices of Doppler flow patterns compared with MRI or angiographic measurements to detect significant coarctation of the aorta. Echocardiography 2002 Jan; 19(1): 55–60.
8. Seifert BL, Des Rochers K, Ta M, et al.: Accuracy of Doppler methods for estimating peak-to-peak and peak instantaneous gradients across coarctation of the aorta: An In vitro study. J Am Soc Echocardiogr 1999 Sep; 12(9): 744–53,
9. Tacy TA, Baba K, Cape EG: Effect of aortic compliance on Doppler diastolic flow pattern in coarctation of the aorta. J Am Soc Echocardiogr 1999 Aug; 12(8): 636–42.
10. Marx GR, Allen HD: Accuracy and pitfalls of Doppler evaluation of the pressure gradient in aortic Coarctation JACC 1986; 8, 616.
11. Marx GR, Geva T: MRI and echocardiography in children: how do they compare? Semin Roengenol, 1998 Jul; 33(3): 281–92.
12. Sanders S: Echocardiography and related techniques in the diagnosis of congenital heart defects. Echocardiography, 1984, 1, 185.
13. Simpson IA, Maciel BC, Moises V, et al.: Cine magnetic resonance imaging and color Doppler flow mapping displays of flow velocity, spatial acceleration, and jet formation: a comparative in vitro study. Am Heart J(1993) 126: 1165–1174.
14. Godart F, Labrot G, Devos P, et al.: Coarctation of the aorta: comparison of aortic dimensions between conventional MR imaging 3D MR angiography and conventional angiography. Eur Radiol (2002) 12: 2034–2039.
15. Amparo E G, Higgins CB, Hricak H, et al.: Aortic Dissection: magnetic resonance imaging . Radiology 1985, 155, 399–406.
16. Boxer RA, Fishman MC, LaCorte MA: Diagnosis and postoperative evaluation of supravalvular aortic stenosis by magnetic resonance imaging. Am. J. Cardiol. 1986; 58, 367–368.
17. Chung T: Assessment of Cardiovascular Anatomy in Patients with Congenital Heart Disease by Magnetic Resonance Imaging Pediatr Cardiol 2000; 21: 18–26.
18. de Roos A, Roest AA: Evaluation of congenital heart disease by magnetic resonance imaging. Eur Radiol. 2000; 10(1): 2–6.
19. Fisher MR, Lipton MJ, Higgins CB: Magnetic resonance imaging and computed tomography in congenital heart disease. Semin Roentgenol (1985) 20: 272–282.
20. Fletcher BD, Jacobstein MD, Nelson AD et al.: Gated magnetic resonance imaging of congenital cardiac malformations. Radiology (1984) 150: 137–140.
21. Ho VB, Kinney JB, Sahn DJ: Contributions of newer MR imaging strategies for congenital heart disease. Radiographics (1996)16: 43–60.
22. Ho VB, Prince MR: Thoracic MR aortography: imaging techniques and strategies. Radiographics. 1998 Mar-Apr; 18(2): 287–309.
23. Kapuściński O, Zaleska T, Walecki J, et al.: Zastosowanie tomogafii rezonansu magnetycznego w rozpoznawaniu chorób aorty (Use of magnetic resonance tomography in diagnostics of aortic diseases – in Polish). Rez. magn. med. 1994, 2, 2, 41–46.
24. Laissy JP, Blanc F, Soyer P, et al.: Thoracic aortic dissection diagnosis with transesophageal echocardiography versus MR imaging. Radiology 1995; 194: 331–336.
25. Riquelme C, Laissy JP, Menegazzo D, et al: MR imaging of Coarctation of the aorta and its postoperative complications in adults: assessment with spin – echo and cine –MR imaging. Magn Reson Imaging (1999) 17: 37–46
26. Stemerman DH, Krinsky GA, Lee VS, et al.: Thoracic Aorta: Rapid Black-Blood MR Imaging with Half-Fourier Rapid Acquisition with Relaxation Enhancement with or without Electrocardiographic Triggering. Radiology 1999; 213: 185–191.
27. Toro-Salazar OH, Steinberger J, Thomas W, et al.: Long term follow-up of Patients After Coarctation of the Aorta Repair. Am J Cardiol 2002; 89: 541–547.
28. Lorenz C.H: The Range of Normal Values of Cardiovascular Structures in Infants, Children, and Adolescents Measured by Magnetic Resonance imaging. Pediatric Cardiol 2000; 21: 37–46.
29. Florentine MS, Grosskreutz CL, Chang W, et al.: Measurement of left ventricular mass in vivo using gated nuclear magnetic resonance imaging. J Am Coll Cardiol 1986; 8: 107–12.
30. Niwa K, Uchishiba M, Aotsuka H, et al.: Measurement of ventricular volumes by cine magnetic resonance imaging in complex congenital heart disease with morphologically abnormal ventricles. Am Heart J (1996) 131: 567–575.
31. Sakuma H, Fujita N, Foo TK, et al.: Evaluation of left ventricular volume and mass with breath-hold cine MR imaging. Radiology (1993) 188:377–380.
32. Helbing WA, de Ross A: Clinical applications of cardiac magnetic resonance imaging after repair of Tetralogy of Fallot. Pediatr Cardiol 2000; 21 70–79.
33. Nollert G, Fischlein T, Bouterwerk S, et al.: Long-term survival in patients with repair of tetralogy of Fallot: 36-year follow-up of 490 survivors of the first year after surgical repair. J Am Coll Cardiol (1997) 30: 1374–1383.
34. Nørgard G, Gatzoulis MA, Josen M, Cullen S et al.: Does restrictive right ventricular physiology in the early postoperative period predict subsequent right ventricular restriction after repair of tetralogy of Fallot? Heart (1998) 79: 481–484.
35. Nørgard G, Gatzoulis MA, Moraes F et al.: Relationship between type of outflow tract repair and postoperative right ventricular diastolic physiology in tetralogy of Fallot. Implications for long-term outcome. Circulation (1996) 94: 3276–3280.
36. Oku H, Shirontani H, Sunakawa A, et al.: Postoperative long-term results in total correction of tetralogy of Fallot: hemodynamics and cardiac function. Ann Thorac Surg (1986) 41: 413–418.
37. Singh GK, Greenberg SB, Yap YS et al.: Right ventricular function and exercise performance late after primary repair of tetralogy of Fallot with the transannular patch in infancy. Am J Cardiol (1998) 81: 1378–1382.
38. Di Cesare E. MRI assessment of right ventricular dysplasia. Eur Radiol. 2003 Jun; 13(6): 1387–93.
39. Di Cesare, E: MRI of the cardiomyopathies. Eur-J-Radiol. 2001 Jun; 38(3): 179–84.
40. Midiri M, Finazzo M: MR imaging of arrhythmogenic right ventricular dysplasia. Int-J-Card-Imaging. 2001 Aug; 17(4): 297–304.
41. Pinamonti B, Sinagra G, Camerini F: Clinical relevance of right ventricular dysplasia/ cardiomyopathy. Heart 2000; 83: 9–11.
42. Laissy JP, Messin B, Varenne O et al.: MRI of acute myocarditis: a comprehensive approach based on various imaging sequences. Chest. 2002 Nov; 122(5): 1638–48.
43. Krasuski RA, Hesselson AB, Landolfo KP et al.: Cardiac rhabdomyomas are extremely uncommon in the adult patient Chest 2000 Oct; 118(4): 1217–21.
44. Wintersperger BJ, Becker CR, Gulbins H et al.: Tumors of the cardiac valves: imaging findings in magnetic resonance imaging, electron beam computed tomography, and echocardiography. Eur Radiol 2000; 10 (3): 443–9.